

# Characterization of Compliant Parallelogram Links for 3D-Printed Delta Manipulators

Pragna Mannam, Oliver Kroemer, and F. Zeynep Temel

**Abstract** We design a compliant delta manipulator using 3D-printing and soft materials. Our design is different from the traditionally rigid delta robots as it is more accessible through low-cost 3D-printing, and can interact safely with its surroundings due to compliance. This work focuses on parallelogram links which are a key component of the delta robot design. We characterize these links over twelve dimensional parameters, such as beam and hinge thickness, and two material stiffness settings by displacing them, and observing the resulting forces and rotation angles. The parallelogram links are then integrated into a delta robot structure to test for delta mechanism behavior, which keeps the end-effector parallel to the base of the robot. We observed that using compliant hinges resulted in near-delta behavior, laying the groundwork for fabricating and utilizing 3D-printed compliant delta manipulators.

## 1 Introduction

Personal care robots operating in homes require dexterous and compliant manipulators to ensure that interactions with human and objects are performed reliably and safely. Delta robots, Figure 1(a), are ideal for these applications due to their low-inertia and high-precision [1]. The dexterity and precision of these robots enable them to manipulate objects in unstructured home environments. However, most delta robots are made from rigid materials [2] which precludes them from interacting safely with humans. The compliance of soft materials, on the other hand, can allow them to conform to objects, exhibit physical robustness, and execute safe human interactions [4]. Furthermore, 3D-printing delta robots using soft materials reduces fabrication costs and makes them accessible to a wider community. This paper presents the process of designing the first 3D-printable compliant delta robot using soft materials. We characterize parallelograms, an integral component of the

---

Carnegie Mellon University, Pittsburgh PA 15213, USA,  
e-mail: {pmannam, okroemer, ztemel}@andrew.cmu.edu

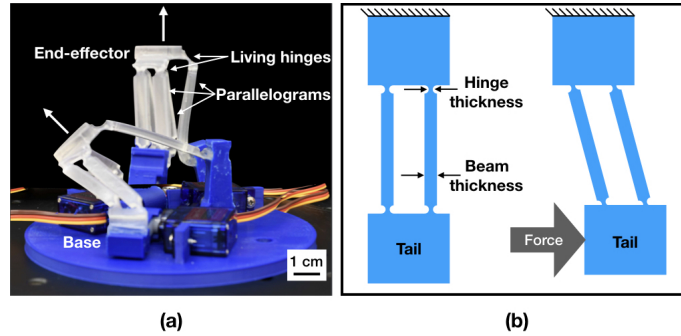


**Fig. 1** (a) A delta robot with each arm consisting of a rigid portion and a flexible parallelogram with living hinges that transfers motion from motors at base to end-effector. (b) Ideal behavior of displaced tail of the parallelogram in characterization experiments testing different hinge and beam thicknesses and materials.

delta robot, with varying dimensional parameters and materials to study their behavior as part of a delta mechanism. More specifically, we focus on parallelogram hinge and beam thicknesses, and material stiffness. These design choices can then be leveraged to achieve desired end-effector behaviors of 3D-printed delta robots composed of compliant parallelogram links.

Printing compliant delta robots requires a departure from the classical delta design due to the use of soft materials, especially with respect to the joints. Rigid universal joints are replaced by two types of living hinges<sup>1</sup>, one in the compliant parallelogram links of the delta robot and the other between the end-effector and the parallelogram links, as seen in Figure 1(a). Properties inherent to soft materials like bending and hysteresis can alter the delta mechanism behavior. As shown in Figure 1(a), we expect the end-effector (or platform) of the delta robot to always stay parallel to its base as seen in the upright position; however, this orientation is not guaranteed in all configurations when using compliant materials. This deviation from the ideal kinematic behavior can be measured by the end-effector rotation with respect to the base across the robot configuration space. In this work, we study the characteristics of centimeter-scaled compliant parallelograms with 12 varied combinations of hinge and beam thicknesses, and 2 materials by displacing them incrementally and observing the force required and resulting rotation of the parallelogram tail, as shown in Figure 1(b). Subsequently, we evaluate these parallelograms by integrating them into the delta robot structure and measuring the end-effector rotation with respect to the base in specific configurations of the robot. These experiments allow us to infer the parameters of the compliant parallelogram link that achieve the ideal kinematic behavior, bringing us one step closer to the goal of creating a 3D-printed compliant delta manipulator.

<sup>1</sup> A **living hinge** is an articulated joint created by locally reducing the width of the material to make it more compliant in that region.

## 2 Related Work

Compliant robots have been used in biomedical applications and are built on micro or milli scale using flexure-based mechanisms. Manufacturing compliant robots on such a small scale is difficult using traditional techniques and are typically built using either Micro Electro Mechanical Systems (MEMS) [5, 7, 8], or Electro-Discharge Machining (EDM) [6, 9, 10, 11]. These manufacturing techniques require sophisticated tools that are not accessible to the wider community. An alternative approach is to utilize origami-inspired self-folding robots [14, 15, 16] or laminate robot mechanisms [17, 5, 13]. Our work is closest to the millimeter-scaled Delta robot using laminate structures [5]. Unlike the manual assembly required for laminate robot mechanisms, we look to successful prototyping of compliant mechanisms using 3D-printing [12]. Our goal is to create a low-cost compliant delta manipulator without using complex manufacturing techniques by relying on 3D-printing.

A popular alternative parallel manipulator is the 6-DOF Stewart platform [3] that can translate and tilt the end-effector unlike the delta robot which only allows the end-effector to translate parallel to the base. Both of these manipulators can move at high speeds and accelerations with low-inertia because their relatively heavy motors are stationary and at the base. Delta robots, unlike Stewart platforms, have simple closed-form kinematic solutions [2]. The characteristics improve as the mechanisms are scaled down, which is why delta robots like the mm-scaled delta (milliDelta) can move with precision down to 5 micrometers in a  $7\text{mm}^3$  workspace and lend themselves to micromanipulation [5]. Previous mm-scaled delta robots required multi-step processes or manual assembly which introduced irregularities in the final platforms [5][13]. In contrast, we use 3D-printing to make repeatable and accessible delta robots.

## 3 Approach

The parallelogram structure plays an integral role in the delta robot's functionality [1]. The key components of the parallelogram are the beam and hinge thicknesses, as labeled in Figure 1(b). Hence, we start with characterizing the parallelograms with varying beam and hinge thicknesses, as well as two different materials, by recording the effect on force and position when displacing the tail of the parallelogram as shown in Figure 1(b). Subsequently, we study the compounding effects of three parallelogram links in a delta robot structure on the resulting end-effector orientation. This enables us to model the mechanical properties of different materials and dimensional parameters of the compliant parallelogram that result in motions close to the idealized delta mechanism.

We characterized and evaluated the parallelogram links over twelve combinations of dimensional parameters: 3 beam thickness values of 2.5mm, 3.5mm and 4.5mm, and hinge thickness values of 0.375mm, 0.5mm, 0.75mm, and 1mm to study deviations from the ideal delta kinematic model caused by different hinge and beam

thicknesses. For our experiments, we used Ultimaker S5 3D-printer and filaments. We chose the two most compliant Ultimaker filament materials which are best suited to living hinge mechanisms, polypropylene (PP) and thermoplastic polyurethane (TPU) 95A. For comparison, the tensile modulus is 220 MPa (using ISO 527) and 26 MPa (using ASTM D638) for PP and TPU respectively. Additionally, the flexural strength is 13 MPa and 4.3 MPa (both measured using ISO 178) for PP and TPU respectively. These values indicate that TPU is more compliant than PP, which is beneficial for the living hinges while the stiffness of PP is useful to maintain rigidity of the parallelogram beams.

### 3.1 Characterization of Parallelogram

The two parameters for characterization experiments were the parallelogram beam and hinge thicknesses (Figure 1(b)). The remaining dimensions were fixed, such as the length and depth of the beams which were 27mm and 4mm respectively, and the length of the hinge was always 2mm. Compliant parallelograms were made from PP and TPU while supporting and mounting materials were 3D-printed using rigid polylactic acid (PLA) material. Characterization experiments involved mounting these parallelograms vertically and using a linear actuator to push the parallelogram tails in 5mm increments to measure the exerted force, and resulting displacement and orientation change of the tails. We vertically mounted parallelograms to reduce the effects of gravity in pulling the parallelogram out of plane. As shown in Figure 2(a), an Actuonix L12-R Micro Linear Servo is mounted with a Transducer Techniques GS0-150 load cell to measure the force required to displace the parallelogram tail. For PP parallelograms with beam thickness of 4.5mm, we used the GS0-500 load cell instead to measure the higher force values that were required to displace these parallelograms. Three grey markers on the parallelogram are tracked as a rigid body by an OptiTrack V120:Trio camera with submillimeter accuracy to record the position and orientation of the parallelogram tail. The load stem was lubricated to overcome frictional effects when pushing the parallelogram. Force measurements were recorded after a six minute delay to allow for stabilization of any creep (deformation) effect. Additionally, rotation data from the markers on the parallelogram indicate if the tail of the parallelogram rotated out-of-plane or twisted in plane.

Using the same reference axes as shown in Figure 2(a), we observe in-plane and out-of-plane rotations of the parallelogram tail. The force applied by the actuator causes the tail of the parallelogram to move in an arc in the plane of the parallelogram. Under ideal conditions, the tail would remain parallel to the base. However, due to non-ideal hinge and beam behaviors, the tail exhibits additional rotations within the plane of movement, i.e., about the Z axis. Additionally, the restorative force of the parallelogram (caused by gravity and joint stiffness) will push back against the actuator. Misalignment between this restorative force and the actuator's pushing force can result in the parallelogram twisting (Y axis rotation) or bending out of

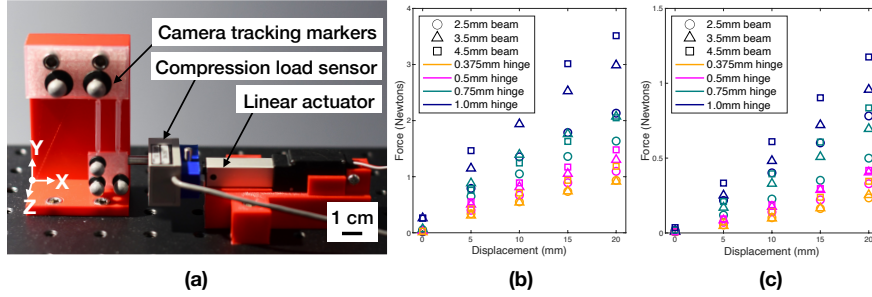


**Fig. 2** (a) Parallelogram characterization experiment setup: linear actuator mounted with compression load sensor to displace the tail of a PP parallelogram with beam thickness = 2.5mm and hinge thickness = 0.375mm. (b) Force-displacement plots for PP and (c) TPU for varying beam thicknesses (shown with shapes) and hinge thicknesses (shown with colors). Each marker represents the mean across five repetitions of the experiment.

plane (X axis rotation). Thus, we only focus on the in-plane rotations to test whether the parallelogram tail stays parallel to the mounted end of the parallelogram.

### 3.2 Evaluation of Delta Mechanism

Rotations of the compliant parallelogram links directly relate to the rotations of the delta robot end-effector. Hence, using the same parallelograms tested in the characterization experiments, we validated the results by integrating the parallelograms as links in an actuated delta robot as shown in Figure 4. The parallelogram links have an added living hinge on each side, oriented 90 degrees apart from the compliant links' revolute joint, to mimic one universal joint at each end of the beams as shown in Figure 1(a). Three of these parallelograms are attached to a triangular end-effector platform, all created with either PP or TPU throughout. Then, the compliant delta tops are secured to 3D-printed rigid links made with Ultimaker Tough PLA (shown in red in Figure 4) which are attached to servo motors.

To measure the end-effector rotation with respect to the base at different configurations of the robot, we define two configurations for each of the arms, namely up and down, that are separated by a 50 degrees offset. We consider two configurations of the robot, one in which two arms are down and the other arm is up, and the other in which two arms are up and the other arm is down. The three marker points on the end-effector are used to calculate the end-effector plane and normal axis. The normal axis is computed at each position of the delta robot, such that the angle between the normal vector and a reference base normal is used to compute the rotation of the end-effector with respect to the base.

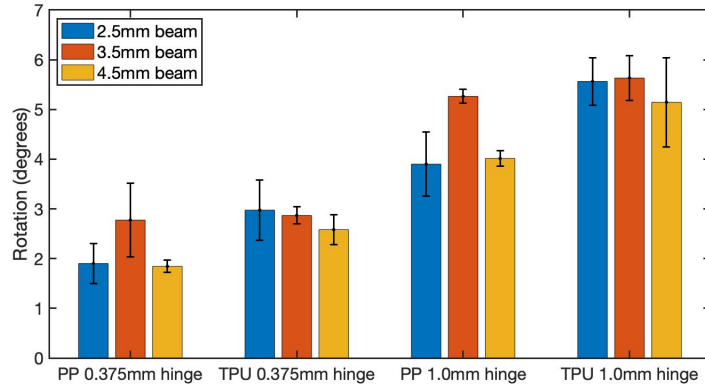


**Fig. 3** Characterization experiment results for Z rotation angles (in degrees) of PP and TPU parallelograms at the largest displacement (20mm). The mean and standard deviation shown as error bars are taken over five repetitions of the experiment. The most compliant hinges (0.375mm) and least compliant hinges (1.0mm) are grouped together, and the colors denote different beam thicknesses of 2.5, 3.5, and 4.5 mm.

## 4 Experimental Results

### 4.1 Characterization experiments

We tested parallelograms of varying hinge thickness (0.375, 0.5, 0.75, and 1mm) with beam thickness of 2.5mm, 3.5mm, and 4.5mm. The force values at the end of each 5mm increment push until 20mm for both PP and TPU, averaged over five repetitions, are shown in Figure 2(b) and (c) respectively. The circle, triangle, and square markers denote 2.5mm, 3.5mm, and 4.5mm respectively, and each color denotes a difference hinge thickness between 0.375 and 1 mm. Five repetitions were executed for a given set of dimensional parameters and material on a newly printed parallelogram, resulting in a total of 120 characterization experiments. There is a clear trend for both materials where displacing the parallelogram by a larger distance takes more force. Overall, PP parallelograms require more force to displace than ones made from TPU, needing almost 4N versus close to 1.5N for the stiffest (thickest) hinges at 20mm displacement.

Using OptiTrack markers, Z rotation angles of the parallelogram tail were recorded after displacements of 5mm increments up to 20mm. In Figure 3, the mean and standard deviation for Z rotation angles are shown for both PP and TPU at the largest (20mm) displacement. For the same beam thickness, increasing the hinge thickness tends to result in larger Z rotations across both materials implying that in-plane rotations are smaller for thinner hinges. We can also observe that for a given beam and hinge thickness, TPU results in larger in-plane rotations when compared to PP. This can be attributed to higher compliance of TPU when compared to PP.

(Beam th., Hinge th.)	X-rotation		Y-rotation		Z-rotation		2 up, 1 down		2 down, 1 up	
	$\mu$	$\sigma$	$\mu$	$\sigma$	$\mu$	$\sigma$	$\mu$	$\sigma$	$\mu$	$\sigma$
PP (2.5, 0.375)	2.31	2.11	2.28	0.85	<b>1.90</b>	0.41	<b>6.27</b>	1.68	<b>5.65</b>	1.66
PP (3.5, 0.375)	1.03	0.38	2.35	1.85	2.78	0.74	8.12	3.80	5.87	1.49
PP (4.5, 0.375)	2.08	0.84	4.68	1.56	<b>1.84</b>	0.12	8.75	2.61	6.15	3.83
PP (2.5, 1.0)	1.20	1.11	3.10	2.65	3.90	0.64	20.08	5.91	17.01	3.31
PP (3.5, 1.0)	1.04	0.38	1.20	0.57	5.26	0.14	15.23	0.86	13.22	1.69
PP (4.5, 1.0)	3.87	1.62	9.32	3.37	4.01	0.16	15.01	0.72	11.57	4.04
TPU (2.5, 0.375)	2.26	1.39	2.06	1.70	<b>2.97</b>	0.61	7.84	3.51	7.69	2.23
TPU (3.5, 0.375)	1.21	1.03	1.41	0.72	<b>2.87</b>	0.17	5.5	0.24	5.44	1.48
TPU (4.5, 0.375)	1.06	1.42	1.60	0.95	<b>2.58</b>	0.30	<b>4.72</b>	1.42	<b>5.00</b>	2.09
TPU (2.5, 1.0)	0.62	0.24	5.86	3.82	5.56	0.48	17.18	4.83	13.55	2.00
TPU (3.5, 1.0)	0.73	0.59	2.03	1.83	5.63	0.45	18.54	5.95	15.35	4.36
TPU (4.5, 1.0)	0.93	0.26	2.50	1.96	5.14	0.90	20.49	9.99	14.67	2.08

**Table 1** Characterization experiment results for X, Y, and Z rotation of parallelograms at 20mm displacement. The mean ( $\mu$ ) and standard deviation ( $\sigma$ ) is taken over five repetitions of the experiment. The last two columns consist of data from evaluation experiments integrating parallelograms of varying beam and hinge thicknesses and calculating the rotation of end effector (in degrees). The mean and standard deviation of three repetitions raising 2 arms and lowering one arm (2 up, 1 down) as well as lowering 2 arms and raising 1 arm (2 down, 1 up) by 50 degrees is listed in fourth and fifth columns respectively.

Interestingly, for a fixed hinge thickness varying the beam thickness does not show consistent behavior across materials and hinge thicknesses. We leave exploring the reasons to future work.

The X, Y, and Z rotation angles with mean and standard deviation at 20mm displacement of the parallelogram can be found in the first three columns of Table 1. As expected from our discussion in Section 3.1, X and Y rotations, corresponding to out-of-plane rotations, have high standard deviations due to misaligned restorative and actuator pushing forces. We have included these rotation values for completeness in Table 1. We can conclude that for both PP and TPU materials, a hinge thickness of 0.375mm results in the least in-plane rotation. For beam thickness, the table indicates that both 2.5mm and 4.5mm for PP material have small in-plane rotations. Similar to Figure 3, we can infer that PP material achieves smaller mean in-plane rotation when compared to TPU material across all settings which can be again attributed to the difference in stiffness between the materials.

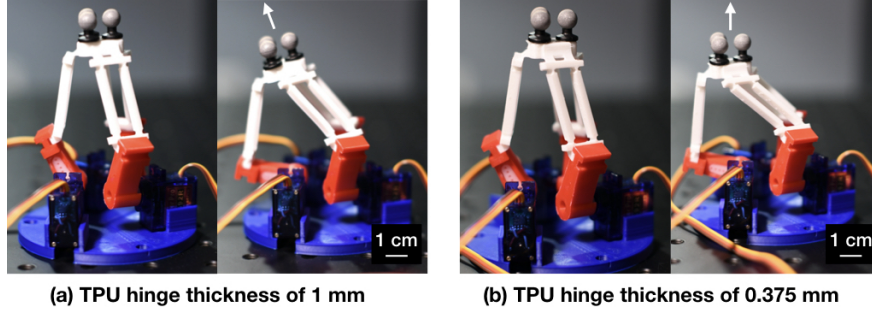


**Fig. 4** Evaluation experiment parallelograms with beam thickness 2.5mm and hinge thickness of (a) 1mm and (b) 0.375mm are shown before and after lowering one arm (2 arms up, 1 down) by 50 degrees.

## 4.2 Evaluation Experiments

We evaluated the effects of integrating parallelograms from the characterization experiments, TPU and PP parallelograms with the most and least compliant hinges (0.375mm and 1.0mm), into full delta mechanisms. Specifically, we studied the effect on the end-effector orientation, relative to the base, when it is moved towards the edge of the configuration space, by lowering or raising each arm by 50 degrees, as shown in Figure 4. Both configurations were repeated three times with each of the three arms. We present the mean and standard deviation of the end-effector rotation in Table 1 (last two columns.) For both PP and TPU materials, hinge thickness of 0.375mm results in a smaller end-effector rotation when compared to a hinge thickness of 1.0mm across all settings. This highlights the importance of compliance in living hinges to achieve delta behavior that is closer to ideal. With a thick hinge, parallelogram links are stiff and unable to maintain the end-effector orientation to be parallel to the base. This is similar to the conclusion drawn from our characterization experiments where we observed that smaller hinge thicknesses are better for minimal in-plane rotations.

Among parallelograms with hinge thickness of 0.375mm, a beam thickness of 2.5mm works best for PP while a beam thickness of 4.5mm works best for TPU. This can be attributed to the stiffness of PP which requires thinner beam to be flexible enough to maintain the end-effector orientation across different configurations. On the other hand, TPU is more compliant and requires thicker beams to ensure that the beams stay parallel to each other which is important to achieve an end-effector orientation that is parallel to the base.

The amount of permissible rotation is dependent on the application, but for manipulating large objects (centimeter scale or larger) 7 degrees of rotation or less is manageable. From a visual perspective as well, about 7 degrees of rotation in Figure 4(b) still demonstrates near-delta robot behavior.



## 5 Conclusion and Future Work

We tested 3D-printed parallelograms made with two materials of significantly varying stiffness, PP and TPU. The characterization experiments presented in Section 4.1 studied the effects of displacing the parallelogram tail. Due to the large variation in amount of force required for each of the parallelogram dimensions and materials, the force profile can be chosen for a specific application. For example, a delta robot that is interacting with humans for applications like assisted feeding is expected to be more compliant and therefore require less force to be displaced. Thus, we can tailor the parameters and material of the parallelogram links to the desired application using the force profile. Our characterization experiments have also indicated that more compliant hinges and PP material are better for achieving minimal in-plane rotations. Our evaluation experiments in Section 4.2 also show that more compliant hinges result in end-effector orientations that are closer to ideal delta behavior. In addition, our evaluation experiments have also provided insight into the ideal beam thickness for PP and TPU materials that result in minimal end-effector rotation.

Working with soft materials is challenging as their properties change over time and across repetitions. In order to control the 3D-printed delta for manipulation, we will have to learn how to accommodate for the material properties and adapt to changes. Our work is an initial step in this direction and the experiments show the potential of a 3D-printed delta using soft materials. Future extensions of this work involve manipulation tasks using opposing delta manipulators, arrays of delta robots for distributed actuation platforms, and modeling compliant delta robots. Modeling the delta robots also involves studying the error from rigid delta kinematic models and how to compensate for the error using robust control and state estimation techniques.

**Acknowledgements** We thank Avi Rudich, Anirudh Vemula, Ankit Bhatia, Tess Hellebrekers, and Keene Chin for their assistance and support. The research presented in this work was funded by National Science Foundation under Grant No. CMMI-2024794 as well as an Amazon Research Award.

## References

1. L. Rey and R. Clavel. The delta parallel robot. In *Parallel Kinematic Machines*, pages 401-417. Springer, 1999.
2. L. Tsai. *Robot Analysis: The Mechanics of Serial and Parallel Manipulators*. (John Wiley & Sons, 1999).
3. D. Stewart. A Platform with Six Degrees of Freedom. *Proceedings of the Institution of Mechanical Engineers*. 180.1 (1965): 371-386.
4. C. Laschi, B. Mazzolai, and M. Cianchetti. "Soft robotics: Technologies and systems pushing the boundaries of robot abilities." *Science Robotics* 1.1 (2016): eaah3690.
5. H. McClintock, F. Z. Temel, N. Doshi, J. Koh, and R. J. Wood. The millidelta: A high-bandwidth, high-precision, millimeter-scale delta robot. *Sci. Robotics*, 3(14), 2018.

6. Y. Tian, et al. "Design and forward kinematics of the compliant micro-manipulator with lever mechanisms." *Precision Engineering* 33.4 (2009): 466-475.
7. N. P. Belfiore, and P. Simeone. "Inverse kinetostatic analysis of compliant four-bar linkages." *Mechanism and Machine Theory* 69 (2013): 350-372.
8. M. Balucani, et al. "The development of a MEMS/NEMS-based 3 DOF compliant micro robot." 19th International Workshop on Robotics in Alpe-Adria-Danube Region (RAAD 2010). IEEE, 2010.
9. U. Bhagat, et al. "Design and analysis of a novel flexure-based 3-DOF mechanism." *Mechanism and Machine Theory* 74 (2014): 173-187.
10. M. L. Culpepper, and G. Anderson. "Design of a low-cost nano-manipulator which utilizes a monolithic, spatial compliant mechanism." *Precision engineering* 28.4 (2004): 469-482.
11. B. J. Yi, et al. "Design and experiment of a 3-DOF parallel micromechanism utilizing flexure hinges." *IEEE Transactions on robotics and automation* 19.4 (2003): 604-612.
12. R. S. Pierre, N. Paul, and S. Bergbreiter. "3DFlex: A rapid prototyping approach for multi-material compliant mechanisms in millirobots." 2017 IEEE International Conference on Robotics and Automation (ICRA). IEEE, 2017.
13. J. E. Correa, et al. 'Laminated micro-machine: Design and fabrication of a flexure-based Delta robot.' *Journal of Manufacturing Processes* 24(2016): 370-375.
14. A. Mehta, J. DelPreto, and D. Rus. "Integrated codesign of printable robots." *Journal of Mechanisms and Robotics* 7.2 (2015).
15. S. J. Kim, et al. "An origami-inspired, self-locking robotic arm that can be folded flat." *Science Robotics* 3.16 (2018).
16. B. Shin, et al. "Self-assembling sensors for printable machines." 2014 IEEE International Conference on Robotics and Automation (ICRA). IEEE, 2014.
17. J. Koh, et al. "A modular folded laminate robot capable of multi modal locomotion." *International Symposium on Experimental Robotics*. Springer, Cham, 2016.